Available online at www.sciencedirect.com
SCIENCE DIRECT®
ELSEVIER
International Journal of Heat and Mass Transfer 47 (2004) 2883–2887
International Journal of HEAT and MASS TRANSFER
www.elsevier.com/locate/ijhmt

Technical Note

A matrix based correction scheme of the liquid fraction during columnar solidification

M. Hainke *, J. Friedrich, G. Müller

Crystal Growth Laboratory, Fraunhofer Institute IISB, Schottkystr. 10, D-91058 Erlangen, Germany

Received 28 February 2003; received in revised form 1 October 2003

Abstract

The derivation of a liquid fraction correction equation for macrosegregation computations entirely on a matrix level is presented. The method is implemented in the software package CrysVUn. The performance of the method is compared to an enthalpy based correction scheme for a solidification benchmark problem.

Keywords: Macrosegregation; Phase diagram coupling; Columnar solidification

---

1. Introduction

Numerical solution of alloy solidification processes requires the coupled solution of heat-, momentum-, mass- and species transfer. One particular task is the coupled solution of the energy and the species conservation equation(s) under the consideration of the phase diagram. Additional difficulties arise due to the lack of an *explicit* equation for the liquid fraction.

Thus, the formulation of suitable coupling schemes has been extensively discussed in literature. An equation for the liquid fraction correction based on the definition of the enthalpy was proposed by Voller et al. [1]. Based on the definition of the mixture concentration, an equation for the liquid fraction is used by Beckermann and Viskanta [2] in the case of local equilibrium, and by Felicelli et al. for non-equilibrium solidification of binary [3,4] and multicomponent alloys [5,6]. A mixture implicit, explicit algorithm was proposed by Swaminathan and Voller [7]. Schneider and Beckermann [8] derived an equation for the liquid fraction, by substitution of the discretized equations for the temperature, species and the phase diagram relationship.

In this work, we present a liquid fraction correction scheme based entirely on the matrix form of the governing equations.

2. Governing equations

The equations for columnar dendritic growth are briefly summarized in the following. A detailed derivation of these equations can be found in [10]. All symbols are explained in the appendix of this note.

The energy conservation equation in terms of the temperature is obtained from the averaged enthalpy conservation equation and reads

$$\frac{\partial}{\partial t}([\rho c_\mathrm{p}]T) + \nabla \cdot (\epsilon_\mathrm{l}\rho_\mathrm{l}c_\mathrm{p,l}\mathbf{v}_\mathrm{l}T) = \nabla \cdot (\lambda \nabla T) - \rho_\mathrm{s}L\frac{\partial \epsilon_\mathrm{l}}{\partial t} \qquad (1)$$

whereby the mixture term on the LHS is defined as

$$[\rho c_\mathrm{p}] = \epsilon_\mathrm{s}\rho_\mathrm{s}c_\mathrm{p,s} + \epsilon_\mathrm{l}\rho_\mathrm{l}c_\mathrm{p,l} \qquad (2)$$

and the mixture conductivity is defined by

$$\lambda = \epsilon_\mathrm{s}\lambda_\mathrm{s} + \epsilon_\mathrm{l}\lambda_\mathrm{l} \qquad (3)$$

The formulation of the species conservation equation requires assumptions on the microsegregation behavior.

---

[*] Corresponding author. Tel.: +49-9131-761-233; fax: +49-9131-761-312.

E-mail address: marc.hainke@iisb.fraunhofer.de (M. Hainke).

URL: http://www.kristallabor.de.

0017-9310/$ - see front matter © 2003 Elsevier Ltd. All rights reserved.
doi:10.1016/j.ijheatmasstransfer.2003.10.039

Nomenclature

a	matrix coefficient
C_l	liquid concentration of a chemical species, wt.pct.
c_p	specific heat, J/kg K
D	diagonal matrix or mass diffusion coefficient, m^2/s
$\mathbf{E}$	matrix, resulting from the discretization of the energy equation
e	matrix coefficient
i	index
j	index
k	index
L	latent heat of phase change, J/kg
m	liquidus line slope, K/wt.pct.
n	iteration counter
ND	off-diagonal matrix
rhsE	vector, resulting from the discretization of the energy equation
rhsS	vector, resulting from the discretization of the species equation
$\mathbf{S}$	matrix, resulting from the discretization of the species equation
T	temperature, K
T_{pure}	pure substance melting point, K
t	time, s
$\mathbf{v}_l$	velocity, m/s

Greek/cal./symbols

$\mathcal{CORR}$	liquid fraction correction matrix
α	under-relaxation factor
Δ	discretized volume or time step
δ	Kronecker symbol or *correction*
$\epsilon_{l,s}$	liquid/solid fraction, $\epsilon_l = 1 - \epsilon_s$
ζ	back diffusion parameter
κ	partition coefficient, wt.pct./wt.pct.
$\lambda_{l,s}$	liquid/solid thermal conductivity, W/Km
$\rho_{l,s}$	liquid/solid mass density, kg/m^3
$\mathscr{E}$	diagonal matrix
$\mathscr{P}$	phase diagram relation
$*$	preliminary value

The two classical limiting cases are given by Scheil's relation (non-equilibrium treatment) and the lever rule (equilibrium treatment). The species conservation equation in terms of the liquid concentration reads

$$\frac{\partial}{\partial t}(\rho_l\epsilon_l C_l + \zeta\rho_s\epsilon_s\kappa C_l) - (1-\zeta)\rho_s\kappa C_l\frac{\partial\epsilon_l}{\partial t} + \nabla\cdot(\epsilon_l\rho_l C_l\mathbf{v}_l) = \nabla\cdot(D\epsilon_l\rho_l\nabla C_l) + C_l(\rho_l - \rho_s\kappa)\frac{\partial\epsilon_s}{\partial t} \tag{4}$$

whereby the parameter $0 \leqslant \zeta \leqslant 1$ lies between the limits of zero back diffusion ($\zeta = 0$) and complete back diffusion ($\zeta = 1$). For a discussion of this parameter, see the recent publication of Voller [11].

A closure relation is provided by the phase diagram, which correlates the temperature and the liquid concentration and reads for a binary system

$$T = T_{\text{pure}} + mC_l \tag{5}$$

3. The correction scheme

Starting point of a numerical solution of Eqs. (1), (4) and (5) is the transformation of the governing equations in an algebraic system. Adopting a fully implicit discretization technique, the energy equation Eq. (1) can be expressed as

$$\mathbf{E}(\epsilon_l)T = \mathbf{rhsE}(\epsilon_l) - \mathscr{E}\cdot(\epsilon_l - \epsilon_l^{\text{old}}) \tag{6}$$

whereby ϵ_l^{old} denotes the value of the liquid fraction at the old time step, the other variables T and ϵ_l are evaluated at the new time step. The matrix $\mathbf{E}$ contains the contributions of the transient-, convective- and diffusive terms of Eq. (1) and the diagonal matrix $\mathscr{E}$ on the RHS is correlated with the evolution of latent heat due to phase change

$$(\mathscr{E})_{i,j} = \rho_s L\frac{\Delta V_i}{\Delta t}\delta_{i,j} \tag{7}$$

The matrix equation for the liquid concentration can be written analogous as

$$\mathbf{S}(\epsilon_l)C_l = \mathbf{rhsS}(\epsilon_l) \tag{8}$$

and the constraint of the phase diagram Eq. (5) can be summarized as

$$T = \mathscr{P}(C_l) \tag{9}$$

The form of the equations above indicate, that the temperature and the concentration can be obtained from Eq. (6) and (8), respectively, whereas no direct equation for the liquid fraction ϵ_l is available. This situation reminds to the numerical solution of the well-known Navier Stokes equations, where the value of the pressure is also only indirectly specified via the constraint of the continuity equation [9,12,13].

As the matrix coefficients themselves do also depend on the unknown value of the liquid fraction (e.g. due to the mixture conductivity Eq. (3)) the solution algorithm requires some sort of iterations. Starting from an initial value (guessed or the value from the old time step) for the liquid fraction ϵ_{l}^*, preliminary solutions for the temperature T^* and the concentration C_{l}^* are obtained. Nevertheless, these solutions (denoted by an asterisk) do normally not satisfy the constraint of the phase diagram

$$T^* \neq \mathscr{P}(C_{\mathrm{l}}^*) \tag{10}$$

This fact is not astonishing, as the phase diagram relation Eq. (9) has not been considered so far in the solution procedure.

To obtain solutions that fulfill the phase diagram constraint Eq. (9), we introduce corrections for the temperature δT

$$T = T^* + \delta T \tag{11}$$

and the concentration δC_{l}, respectively,

$$C_{\mathrm{l}} = C_{\mathrm{l}}^* + \delta C_{\mathrm{l}} \tag{12}$$

Substitution of Eqs. (11) and (12) in Eq. (9) yields a correlation of the temperature and the concentration correction

$$T^* + \delta T = \mathscr{P}(C_{\mathrm{l}}^* + \delta C_{\mathrm{l}}) \tag{13}$$

The only degree of freedom to fulfill Eq. (13), is to change the value of the liquid fraction

$$\epsilon_{\mathrm{l}} = \epsilon_{\mathrm{l}}^* + \delta\epsilon_{\mathrm{l}} \tag{14}$$

The correlations between the correction $\delta\epsilon_{\mathrm{l}}$ of the liquid fraction and the corrections of the temperature δT and the concentration δC_{l} are derived in the following.

An equation, correlating the temperature correction with the liquid fraction correction, can be derived by substracting the energy equation Eq. (6) defined with the preliminary (asterisk) values

$$\mathbf{E}(\epsilon_{\mathrm{l}}^*)T^* = \mathbf{rhsE}(\epsilon_{\mathrm{l}}^*) - \mathscr{E}\cdot(\epsilon_{\mathrm{l}}^* - \epsilon_{\mathrm{l}}^{\mathrm{old}}) \tag{15}$$

from the final energy equation, which gives

$$\mathscr{E}\delta\epsilon_{\mathrm{l}} = \mathbf{rhsE}(\epsilon_{\mathrm{l}}) - \mathbf{rhsE}(\epsilon_{\mathrm{l}}^*) + \mathbf{E}(\epsilon_{\mathrm{l}}^*)T^* - \mathbf{E}(\epsilon_{\mathrm{l}})T \tag{16}$$

The equation is non-linear in the liquid fraction, due to the dependency of the matrix coefficients on the liquid fraction. Progress is made after linearization of the terms $\mathbf{rhsE}(\epsilon_{\mathrm{l}})$ and $\mathbf{E}(\epsilon_{\mathrm{l}})$, reading

$$\begin{aligned}\mathscr{E}\delta\epsilon_{\mathrm{l}} = {} & \mathbf{rhsE}(\epsilon_{\mathrm{l}}^*) + \frac{\partial\mathbf{rhsE}}{\partial\epsilon_{\mathrm{l}}}\delta\epsilon_{\mathrm{l}} - \mathbf{rhsE}(\epsilon_{\mathrm{l}}^*) + \mathbf{E}(\epsilon_{\mathrm{l}}^*)T^* \\ & - \left(\mathbf{E}(\epsilon_{\mathrm{l}}^*) + \left[\frac{\partial\mathbf{E}}{\partial\epsilon_{\mathrm{l}}}\circ\delta\epsilon_{\mathrm{l}}\right]\right)T\end{aligned} \tag{17}$$

whereby a coefficient in the second matrix within parathesis on the RHS is given by

$$e_{i,j} = \sum_k \frac{\partial a_{i,j}}{\partial\epsilon_{\mathrm{l,k}}}\delta\epsilon_{\mathrm{l,k}} \tag{18}$$

After re-arrangement and substitution of Eq. (11) we arrive at

$$\left(\frac{\partial\mathbf{rhsE}}{\partial\epsilon_{\mathrm{l}}} - \left[\left(\frac{\partial\mathbf{E}}{\partial\epsilon_{\mathrm{l}}}\right)^{\dagger}\circ(T^* + \underline{\delta T})\right] - \mathscr{E}\right)\delta\epsilon_{\mathrm{l}} = \mathbf{E}(\epsilon_{\mathrm{l}}^*)\delta T \tag{19}$$

whereby the underscored term is neglected in the following, because it is of second order in the corrections and thus becomes zero more rapidly than the other terms. Note that the second matrix on the LHS is a short-hand notation for

$$e_{i,j}^{\dagger} = \sum_j \frac{\partial a_{i,j}}{\partial\epsilon_{\mathrm{l,i}}}T_j^* \tag{20}$$

Eq. (19) relates the correction δT of the temperature to the correction $\delta\epsilon_{\mathrm{l}}$ of the liquid fraction.

A corresponding equation, which relates the correction of the species δC_{l} to the correction $\delta\epsilon_{\mathrm{l}}$ of the liquid fraction, is derived following the same lines and reads

$$\left(\frac{\partial\mathbf{rhsS}}{\partial\epsilon_{\mathrm{l}}} - \left[\left(\frac{\partial\mathbf{S}}{\partial\epsilon_{\mathrm{l}}}\right)^{\dagger}\circ\left(C_{\mathrm{l}}^* + \underline{\delta C_{\mathrm{l}}}\right)\right]\right)\delta\epsilon_{\mathrm{l}} = \mathbf{S}(\epsilon_{\mathrm{l}}^*)\delta C_{\mathrm{l}} \tag{21}$$

The underscored term is neglected again, for the same reasons as already discussed in the case of the temperature correction Eq. (19).

It can be concluded so far, that we obtained an expression for the nodal temperature correction in terms of the liquid fraction correction, which is formally expressed as

$$\delta T = \delta\widetilde{T} + \mathbf{E}_D^{-1}(\epsilon_{\mathrm{l}}^*)\left(\frac{\partial\mathbf{rhsE}}{\partial\epsilon_{\mathrm{l}}} - \left[\left(\frac{\partial\mathbf{E}}{\partial\epsilon_{\mathrm{l}}}\right)^{\dagger}\circ T^*\right] - \mathscr{E}\right)\delta\epsilon_{\mathrm{l}} \tag{22}$$

with

$$\delta\widetilde{T} = -\mathbf{E}_D^{-1}(\epsilon_{\mathrm{l}}^*)\mathbf{E}_{\mathrm{ND}}(\epsilon_{\mathrm{l}}^*)\delta T \tag{23}$$

as well as for the nodal concentration correction in terms of the liquid fraction correction, which is formally expressed as

$$\delta C_{\mathrm{l}} = \delta\widetilde{C}_{\mathrm{l}} + \mathbf{S}_D^{-1}(\epsilon_{\mathrm{l}}^*)\left(\frac{\partial\mathbf{rhsS}}{\partial\epsilon_{\mathrm{l}}} - \left[\left(\frac{\partial\mathbf{S}}{\partial\epsilon_{\mathrm{l}}}\right)^{\dagger}\circ C_{\mathrm{l}}^*\right]\right)\delta\epsilon_{\mathrm{l}} \tag{24}$$

with

$$\delta\widetilde{C}_{\mathrm{l}} = -\mathbf{S}_D^{-1}(\epsilon_{\mathrm{l}}^*)\mathbf{S}_{\mathrm{ND}}(\epsilon_{\mathrm{l}}^*)\delta C_{\mathrm{l}} \tag{25}$$

The values on the RHS for the temperature correction $\delta\widetilde{T}$ and the concentration correction $\delta\widetilde{C}_{\mathrm{l}}$, which are correlated with the off-diagonal terms of the corresponding matrices, are unknown at this point and will be therefore neglected in the following.

The final step is the substitution of Eqs. (22) and (24) into Eq. (13). This gives after re-arrangement the correction equation for the liquid fraction

$$\mathcal{CORR} \cdot \delta\epsilon_l = T^* - (T_{\text{pure}} + mC_l^*) \tag{26}$$

whereby

$$\mathcal{CORR} = \mathbf{E}_D^{-1}(\epsilon_l^*)\left(\left[\left(\frac{\partial \mathbf{E}}{\partial \epsilon_l}\right)^{\dagger} \circ T^*\right] + \mathscr{E} - \frac{\partial \mathbf{rhsE}}{\partial \epsilon_l}\right) - m\mathbf{S}_D^{-1}(\epsilon_l^*)\left(\left[\left(\frac{\partial \mathbf{S}}{\partial \epsilon_l}\right)^{\dagger} \circ C_l^*\right] - \frac{\partial \mathbf{rhsS}}{\partial \epsilon_l}\right) \tag{27}$$

Eqs. (26) and (27) are the central equations of the matrix based correction scheme. The deviation of the preliminary values from the phase diagram, expressed on the RHS of Eq. (26), acts as the driving force for the liquid fraction correction. In the case of a converged solution, the correction is zero.

On setting $\mathcal{CORR} = \mathbf{E}_D^{-1}(\epsilon_l^*) \cdot \mathscr{E}$ and taking only into account the transient term of Eq. (6) in the matrix $\mathbf{E}_D$, the liquid fraction correction reduces to the correction equation of the enthalpy based algorithm [1], which reads for a constant density

$$\delta\epsilon_l = \frac{c_p}{L}(T^* - (T_{\text{pure}} + m \cdot C_l^*)) \tag{28}$$

Eqs. (26) or (28) may be used in a phase diagram coupling algorithm. Starting with the initial guesses T^{n-1}, C_l^{n-1} and ϵ_l^{n-1}, a simple coupling algorithm is given by [7]

Step 1 solve energy Eq. (15) → T^*
Step 2 solve species Eq. (8) → C_l^*
Step 3 correct liquid fraction with Eq. (26) or (28) → ϵ_l^n

Usually a post-correction step is applied afterwards, reading

Step 4 correct species concentration with Eq. (8) → C_l^n
Step 5 correct temperature inside the mushy zone with Eq. (9) → T^n

These steps are repeated until some convergence criteria are reached. In this work we use the norm of the residuum of Eq. (15) and the relative change of the liquid fraction $\|\epsilon_l^n - \epsilon_l^{n-1}\|/\|\epsilon_l^{n-1}\|$. As usual, an under-relaxation factor α_{ϵ_l} for the liquid fraction correction in step 3 is used.

The coupling scheme is implemented in the software package CrysVUn which is especially designed for the global modeling of solidification processes [14]. For the discretization of the governing equations, the finite volume technique is applied in conjunction with unstructured meshes.

4. Test case

The solidification benchmark published by Ahmad et al. [15] is chosen to investigate the efficiency of the different correction schemes. The test problem considers directional solidification of a Sn–5%Pb alloy in a two-dimensional rectangular area. For more details the reader is referred to the original literature.

For the validation of the coupling algorithm, calculations were first performed without macrosegregation (by setting the viscosity to an arbitrary high value). As can be seen from Fig. 1, the computed temperature liquid fraction relations agree well with the analytical relations for both microscopic limits [16].

The test computations are performed on a grid with approximately 1700 degrees of freedom for each scalar value, the time step is set to $dt = 0.05$ s. A homogeneous temperature field slightly above the liquidus temperature and a zero velocity field are set as initial values. The simulations are stopped after 400 s. Here, nearly the complete computational domain is in the semi-solid state. As convergence criteria within a time step, the norm of the residuum of Eq. (15) is required to be smaller than 5×10^{-7}, the relative change of the liquid fraction is required to be smaller than 1×10^{-7}. To evaluate the coupling methods, the total number of iterations within the coupling algorithm is recorded during the computations.

The results using the under-relaxation values $\alpha_{\epsilon_l} = 0.55$ for both correction schemes are shown in Fig. 2. Here, the matrix based scheme clearly gives the best performance. The average number of required iterations per time step is 5.4, whereas for the enthalpy based scheme, 9.3 iterations per time step are needed in the average.

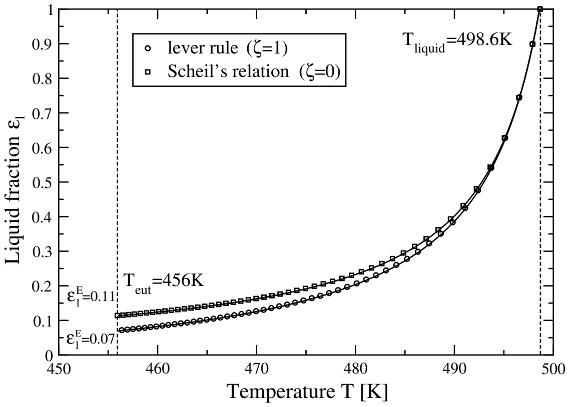

Fig. 1. Liquid fraction vs. temperature in the case of no macrosegregation. Shown are the numerical results (symbols) compared to the analytical solutions (lines) for the microscopic limits of no- ($\zeta = 0$) and infinite ($\zeta = 1$) diffusion.

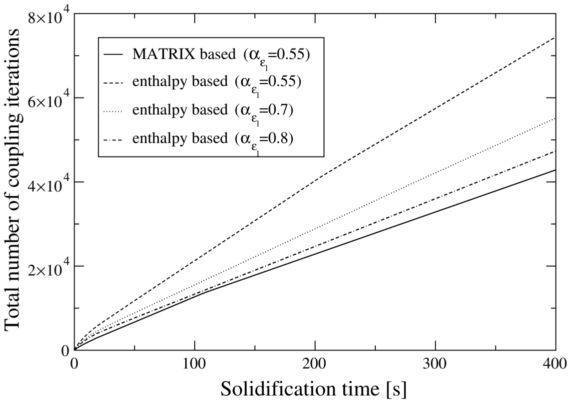

Fig. 2. Total number of required coupling iterations vs. the solidification time.

Nevertheless, the convergence of the coupling schemes is strongly dependent on the under-relaxation parameters used in the calculations. As shown in Fig. 2, the iterations required with the enthalpy based algorithm reduce to the number of iterations needed with matrix based algorithm by using higher values for α_{ϵ_l}. In contrast, using higher under-relaxation factors in the case of Eq. (26) lead to divergence of the computations. In the case of the enthalpy based scheme divergence was resulting using under-relaxation factors higher than $\alpha_{\epsilon_l} = 0.9$.

5. Summary

The derivation of a liquid fraction correction equation is presented, which is based on the matrix form of the discretized equations governing alloy solidification. The equation may be interpreted as an extension of the enthalpy based solution concept [1]. Test computations showed, that the performance of the matrix based scheme can be superior to the enthalpy based method. However, using different numerical parameters the enthalpy based approach results in the same performance. As the implementation of the latter method is much simpler, it can be concluded that the effort of the implementation of the matrix based scheme is not obligatory. Nevertheless, the efficiency may also vary case by case, dependent on the problem under consideration.

Acknowledgements

The authors acknowledge the support of the DLR under contract no. 50WM0042 and the support of ESA under contract no. 14347/00/NL/SH within the framework of the MICAST project.

References

[1] V. Voller, A. Brent, C. Prakash, The modelling of heat, mass and solute transport in solidification systems, Int. J. Heat Mass Transfer 32 (9) (1989) 1719–1731.

[2] C. Beckermann, R. Viskanta, Double-diffusive convection during dendritic solidification of a binary mixture, Physicochem. Hydrodyn. 10 (2) (1988) 195–213.

[3] S. Felicelli, J. Heinrich, D. Poirier, Numerical model for dendritic solidification of binary alloys, Numer. Heat Transfer, Part B 23 (1993) 461–481.

[4] S. Felicelli, J. Heinrich, D. Poirier, Simulation of freckles during vertical solidification of binary alloys, Metall. Trans. B 22B (1991) 847–859.

[5] S. Felicelli, D. Poirier, J. Heinrich, Macrosegregation patterns in multicomponent Ni-base alloys, J. Cryst. Growth 177 (1997) 145–161.

[6] S. Felicelli, D. Poirier, A. Giamei, J. Heinrich, Simulating convection and macrosegregation in superalloys, JOM (1997) 21–25.

[7] C. Swaminathan, V. Voller, Towards a general numerical scheme for solidification systems, Int. J. Heat Mass Transfer 40 (12) (1997) 2859–2868.

[8] M. Schneider, C. Beckermann, Formation of macrosegregation by multicomponent thermosolutal convection during solidification of steel, Metall. Trans. A 26A (1995) 2373–2388.

[9] S. Patankar, D. Spalding, A calculation procedure for heat, mass and momentum transfer in three-dimensional parabolic flows, Int. J. Heat Mass Transfer 15 (1972) 1787–1806.

[10] D. Poirier, P. Nandapurkar, S. Ganesan, The energy and solute conservation equations for dendritic solidification, Metall. Trans. B 22B (1991) 889–900.

[11] V. Voller, On a general back-diffusion parameter, J. Cryst. Growth 226 (2001) 562–568.

[12] J. Ferzinger, M. Perić, in: Computational Methods for Fluid Dynamics, vol. 2, Springer, 1999.

[13] S. Patankar, Numerical heat transfer and fluid flow, Hemisphere Publishing Corporation, 1980.

[14] M. Kurz, Development of CrysVUN++, a software system for numerical modelling and control of industrial crystal growth processes, Ph.D. thesis, Technical Faculty of the University Erlangen-Nürnberg, 1998.

[15] N. Ahmad et al., Numerical simulation of macrosegregation: a comparison between finite volume method and finite element method predictions and a confrontation with experiments, Metall. Trans. A 29A (1998) 617–630.

[16] W. Kurz, D.J. Fisher, Fundamentals of Solidification, Trans. Tech. Publications, 1986.